Experiments on Ignition of Zirconium-Alloy in Prototypical Pressurized Water Reactor Fuel Assemblies in a Spent Fuel Pool with Complete Loss of Coolant

Robert Beaton, Alexander Velazquez-Lozada, Abdelghani Zigh
U.S. Nuclear Regulatory Commission, Washington DC 20555-0001

Sam Durbin and Eric Lindgren
Sandia National Laboratories, Albuquerque, NM 87185

ABSTRACT

This article summarizes an international effort to study zirconium-alloy fire propagation in pressurized water reactor spent fuel pools during complete loss-of-coolant conditions. This international effort was established with the Organisation for Economic Cooperation and Development (OECD) and included the following 13 countries: Czech Republic, France, Germany, Hungary, Italy, Japan, Norway, Republic of Korea, Spain, Sweden, Switzerland, United Kingdom, and the United States (with the U.S. Nuclear Regulatory Commission (NRC) acting as the operating agency).

The experimental program was conducted at Sandia National Laboratories (SNL). The first phase of the program focused on axial heating and burn propagation in a single pressurized-water reactor fuel assembly, and the second phase focused on radial and axial heating and zirconium fire propagation, including the effects of fuel rod ballooning in a 1×4 assembly configuration. The first two sections of this article summarize the background and objectives of the experiments. The subsequent sections describe the testing approach and results of the experimental program.

1. Introduction

Prior to 2001, the NRC performed an evaluation of the potential accident risk in a spent fuel pool (SFP) at decommissioning plants in the United States. NUREG-1738, "Technical Study of Spent Fuel Pool Accident Risk at Decommissioning Nuclear Power Plants," describes a modeling approach for the following:

- a typical decommissioning plant with design assumptions and industry commitments
- the thermal-hydraulic analyses performed to evaluate spent fuel stored in the SFP at decommissioning plants
- the risk assessment of SFP accidents
- the consequence calculations
- the implications for decommissioning regulatory requirements

Some of the assumptions in the accident progression in NUREG-1738 were known to be necessarily conservative, especially the estimation of the fuel damage. The SFP accident research continued by applying best estimate computer codes to predict the severe accident

progression following various postulated accident initiators. The best-estimate computer code studies identified various modeling and phenomenological uncertainties that prompted a need for experimental confirmation.

From 2003 to 2012, the NRC undertook an experimental program to address thermal-hydraulic conditions and zirconium fire propagation during a complete loss of coolant in a boiling-water reactor (BWR) SFP. The results from this study are documented in NUREG/CR-7143, "Characterization of Thermal-Hydraulic and Ignition Phenomena in Prototypic, Full-Length Boiling Water Reactor Spent Fuel Pool Assemblies after a Postulated Complete Loss-of-Coolant Accident," and NUREG/CR-7144, "Laminar Hydraulic Analysis of a Commercial Pressurized Water Reactor Fuel Assembly."

In May 2009, 12 countries from OECD, the Nuclear Energy Agency (NEA), and the NRC signed an agreement called the "OECD/NEA Sandia Fuel Project—An Experimental Programme and Related Analyses for the Characterization of Hydraulic and Ignition Phenomena of Prototypic Water Reactor Fuel Assemblies." The signatories, jointly with NRC, defined an experimental test matrix, experimental conditions, and parameters to be investigated. The objective was to perform a highly detailed thermal-hydraulic characterization of full-length commercial fuel assembly mockups to provide data for the direct validation of severe accident codes. Code predictions based on previous results indicated that fuel assemblies can ignite and radially propagate in an SFP with a complete loss of coolant. Hence, qualified data obtained in representative fuel configurations were needed to confirm these results. The proposed experiments focused on thermal-hydraulic and zirconium fire phenomena in pressurized-water reactor (PWR) assemblies and supplemented earlier results obtained for BWR assemblies. Ignition of the zirconium cladding occurs as it oxidizes with air. This reaction is exothermic and results in significant heat generation. Zirconium oxidation with air releases more heat than with steam and forms nonprotective oxide scales.

The participants believe that code validations based on both the PWR and BWR experimental results will considerably enhance the code applicability to other fuel assembly designs and configurations. Signatories of the agreement have implemented plans to conduct assessments of accident conditions that can arise in spent fuel pools and water reactor cores with complete loss-of-cooling water, resulting in fuel assembly heatup and zirconium-alloy ignition. These plans necessitate the production of data by means of experiments in specialized facilities located at the SNL facility, a U.S. Government-owned and contractor-operated facility located in Albuquerque, NM. The experiments conducted thus far at SNL using prototypical materials and simulating fuel ignition phenomena have produced highly valuable data. Furthermore, the MELCOR code validations serve an important NRC regulatory purpose since MELCOR analyses of severe accidents inform multiple regulatory applications, such as regulatory cost-benefit analyses and environmental impact statements.

2. Objective

The objective of this project was to provide basic thermal-hydraulic data associated with PWR SFP complete loss-of-coolant conditions. The accident conditions of interest for the SFP were simulated in a full-scale prototypic fashion (electrically heated, prototypic assemblies in a prototypic SFP rack) so that the experimental results closely represent actual fuel assembly responses. The major motivation for this work was to facilitate severe accident code validation (ATHLET-CD, ASTEC, DRACCAR, and MELCOR) and reduce modeling uncertainties within the codes.

3. Testing Approach

The study was conducted in two phases. Phase 1 focused on axial heating and burn propagation, while Phase 2 addressed axial and radial heating and burn propagation, including effects of fuel rod ballooning. For each phase, testing included unheated flow tests, pre-ignition tests, and a final destructive ignition test. The unheated flow tests used forced flow into the assemblies to determine pressure drop as a function of the flow velocity. Curve fits to the pressure drop data as a function of the flow velocity through the bundle were used to compute frictional and inertial flow resistance coefficients for use in severe accident analysis codes. The researchers performed pre-ignition tests in which the assemblies were heated using a uniform axial power profile with electrically heated rods to simulate decay power. The key outputs from the pre-ignition tests are the resulting temperatures throughout the assembly and the induced air flow rate. The peak temperatures were kept below a certain value to avoid excessive oxidation of the zirconium components. Each phase concluded with a destructive ignition test in which the assembly was allowed to heat up until the point of ignition and remain burning until the assembly was completely destroyed.

Figure 1 shows a single full-length test assembly constructed with a prototypic fuel skeleton and zirconium-alloy clad heater rods, which represents a commercial 17x17 rod PWR fuel assembly. The main structural component of the assembly is the core skeleton, which consists of 11 spacers attached to 24 guide tubes, one instrument tube, and 264 fuel rods passing through the spacers and held captive in the assembly by the top bus plates and bottom nozzle. Note that the zirconium used for the fuel rods was not pre-oxidized as would be the case of actual spent fuel. For these tests, researchers replaced the top nozzle with a specially designed set of electrical bus plates to allow the application of power into the assembly. As demonstrated in the previous study for BWRs, compacted magnesium oxide (MgO) powder—used to make the electric heater—has a thermal mass similar to uranium dioxide (UO_2) and is an excellent surrogate for spent fuel. The test assemblies were fully instrumented. Researchers used a hot wire anemometer to measure the inlet flow rate to the test assemblies. They made Laser Doppler anemometry measurements mid-bundle between the debris catcher and the first spacer to provide average velocity profiles. Thermocouples were installed throughout the assembly to measure thermal response. Other instrumentation included oxygen sensors, mass spectrometer (argon and nitrogen gas quantification), pressure transducers, and quartz light pipes for visual observation of ignition propagation.

Phase 1 examined a single PWR fuel assembly in two different-sized storage cells that represent commercially available storage cell sizes. The single test assembly was completely insulated to model boundary conditions representing a “hot neighbor” loading pattern, which is a typical bounding scenario. Phase 1 examined where inception of ignition within the assembly first occurs and the nature of the burn in the axial direction of the assembly. Researchers performed separate effect flow tests and pre-ignition testing at seven different power levels using both storage cell sizes. The single ignition test was performed with the larger-sized storage cell (cell 2).

Phase 2 used five full-length assemblies, in which the center assembly was of the same heated design as used in Phase 1, and the four peripheral assemblies were unheated, representing older spent fuel. All mock fuel assemblies were constructed with zirconium alloy cladding and prototypic structural components, as was done in Phase 1. The fuel assemblies were arranged in a pool rack with the heated assembly in the center cell (see Figure 2). These boundary conditions experimentally represent a “cold neighbor” situation that complements the bounding scenario covered by Phase 1. The unheated peripheral fuel rods are filled with high-density

MgO ceramic pellets sized to precisely match the thermal mass of spent fuel. Fuel rods in two of the four peripheral assemblies were pressurized with argon gas (at different pressures) so that these fuel rods would balloon when the zirconium-alloy cladding reached a high enough temperature. The two peripheral assemblies without pressurized rods were used to compare and evaluate the effects of ballooning. Similarly, this phase started with separate effects tests, including unheated hydraulic forced flow tests and pre-ignition tests at eight different power levels. Studies using this test configuration concluded with a final destructive test in which the center assembly was heated until ignition occurred.

Figure 1. Single fuel assembly for Phase 1 testing in the construction stage

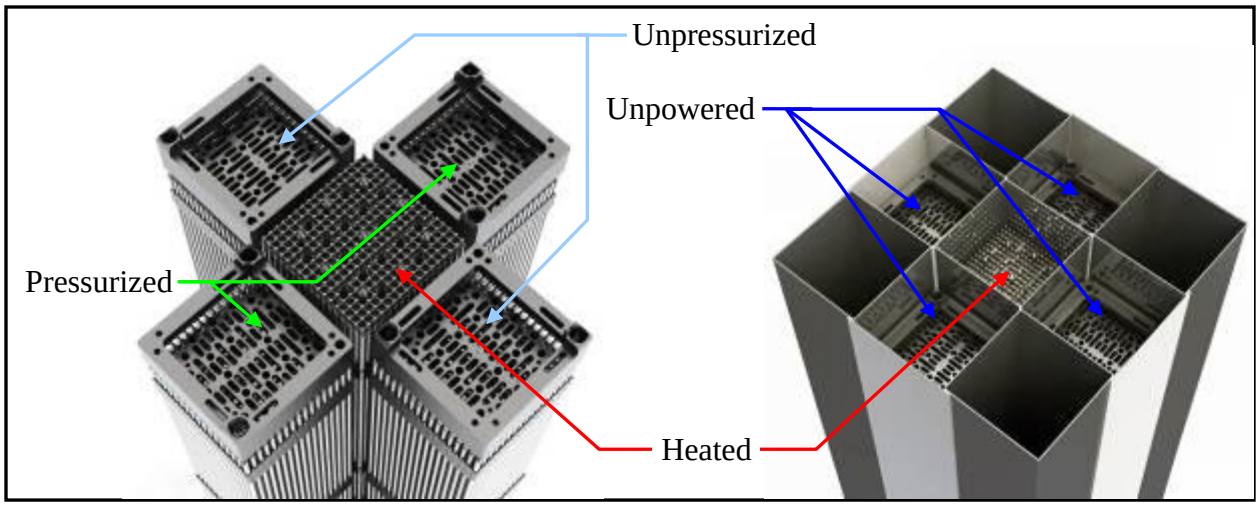

Figure 2. Layout of the Phase 2 test assembly

4. Results

All stages of testing use MELCOR modeling results. Researchers used pretest MELCOR modeling results to guide the experimental test assembly design and instrumentation. MELCOR modeling results were used to choose experimental operating parameters, such as the applied assembly power. At each step in the testing, improvements were made to the MELCOR model to continually increase confidence in the modeling validity. The final version of MELCOR used for the Phase 2 analysis was a developmental version containing features not yet available in a production version of the code. The focus of the MELCOR post-test analysis is the correct prediction of key figures of merit, including time and location of ignition, peak cladding temperatures (PCTs), and burn propagation. Because of the sensitivity of this testing program and in accordance with the OECD/NEA project agreement, all results are presented using normalized data. Note that all MELCOR results presented below are from analysis performed by the NRC. The other countries participating in this program performed their own analysis using either MELCOR or other codes (ATHLET-CD, ASTEC, CFD, DRACCAR, etc.).

The majority of the participants in the project participated in benchmarking exercises for both Phase 1 and Phase 2. These exercises were performed to evaluate and compare the predictive capabilities of severe accident computer codes. The exercises focused on the correct prediction of the onset of zirconium fire parameters (i.e., time and location of ignition, peak cladding temperature, and heat balances). The main objectives of the benchmarks were to assess the current capabilities of the codes on the domains of interest, to develop a common understanding, promote an exchange of knowledge, and to draw conclusions on the possible use of the codes for regulatory bodies and industry.

4.1 Phase 1 results and analysis

Researchers successfully performed the Phase 1 pre-ignition tests and the experimental data compared to MELCOR results. The MELCOR input model was configured with 12 axial nodes and 1 radial core ring, allowing axial and radial radiative heat exchange. Researchers ran MELCOR calculations with current best practice modeling parameters and sensitivity coefficients for the analysis of severe accidents. Figure 3 shows a comparison of the resulting temperature at the end of the experiment for both experimental data and MELCOR for all

pre-ignition testing using cell 2 at a normalized height of 0.804. The MELCOR results agree very favorably with the experimental data. Figure 4 shows a comparison of the induced buoyancy driven air flow rates. The MELCOR model compares very favorably with the measured flow rate to within the uncertainty of the experimental data for all power levels.

Phase 1 of the project concluded with the ignition of the test assembly in the Cell 2 configuration. Researchers conducted this test on March 1, 2011. Figure 5 compares normalized peak cladding temperature as a function of normalized time for the experiment, and that predicted by MELCOR. The experimental data values are truncated beyond the time of ignition because of loss of instrumentation and noise in the remaining thermocouples. The MELCOR calculation of ignition time agreed very favorably with the observed ignition time. Figure 6 compares the volumetric flow between the experimental data and MELCOR. MELCOR captures the trend of the flow as the accident progresses and ignition occurs, and it is within the uncertainty of the experimental data.

During the ignition test, researchers used a residual gas analyzer (RGA) to monitor the amount of nitrogen and argon exiting the top of the assembly. The ratio of nitrogen to argon was used to determine if nitrogen was being consumed by reaction with zirconium. While encountering some sampling difficulties, the RGA successfully measured a significant amount of nitrogen consumption at the start of ignition and during the burn front progression to the bottom of the assembly. During the burn phase, all of the oxygen was removed from the air drawn into the assembly converting some of the initial zirconium to zirconium dioxide (ZrO_2). In addition, some of the zirconium in the assembly was converted to zirconium nitride (ZrN). The test results indicate that the hot oxygen-starved environment remaining after the passage of the burn front is ideal for significant zirconium nitride formation.

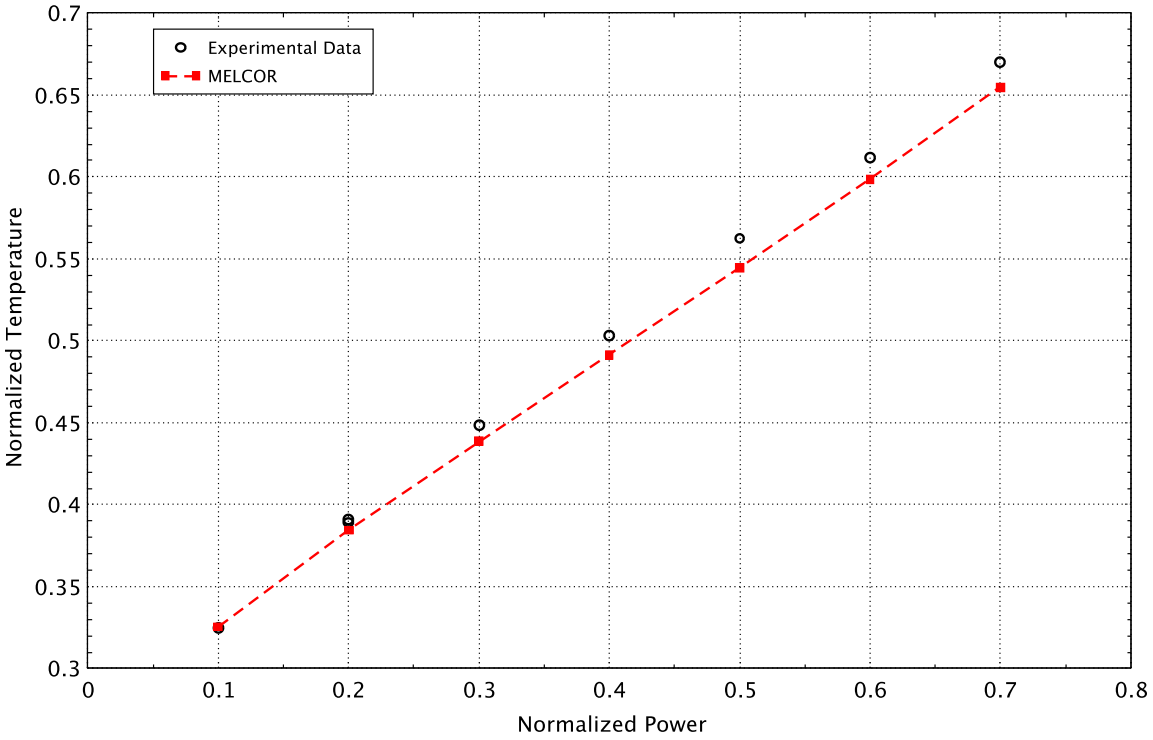

Figure 3. Temperature versus power for the Phase 1 pre-ignition tests using cell 2

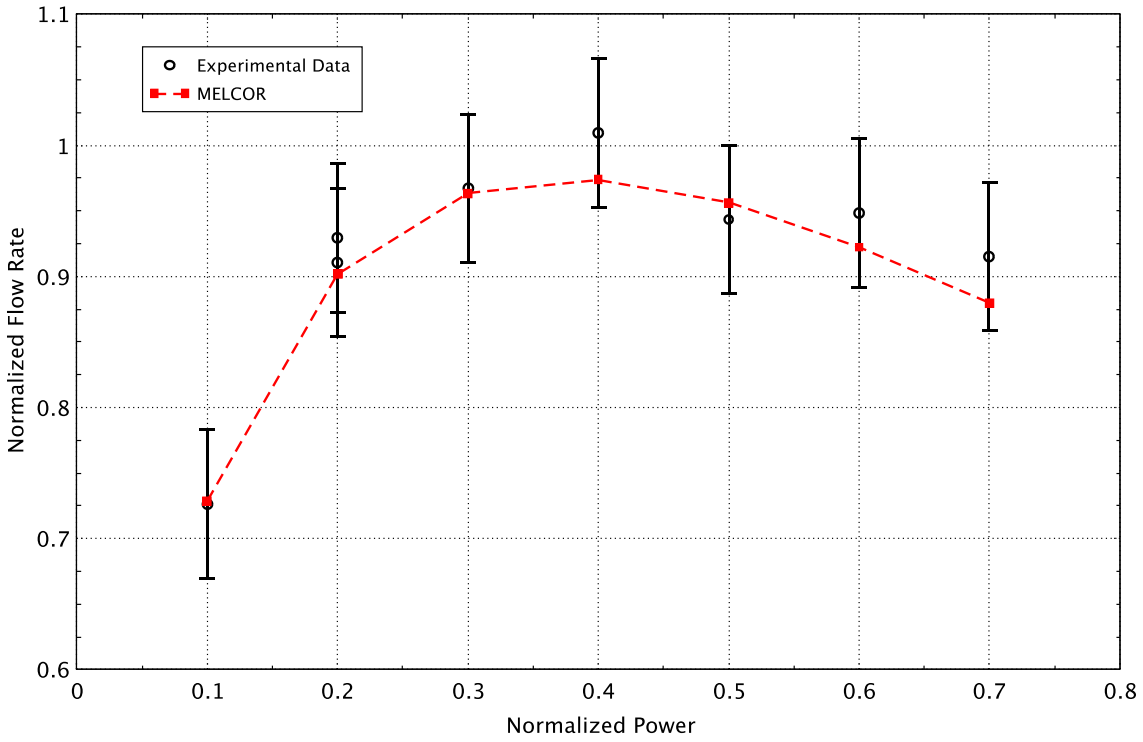

Figure 4. Volumetric flow rate versus power for the Phase 1 pre-ignition tests using cell 2

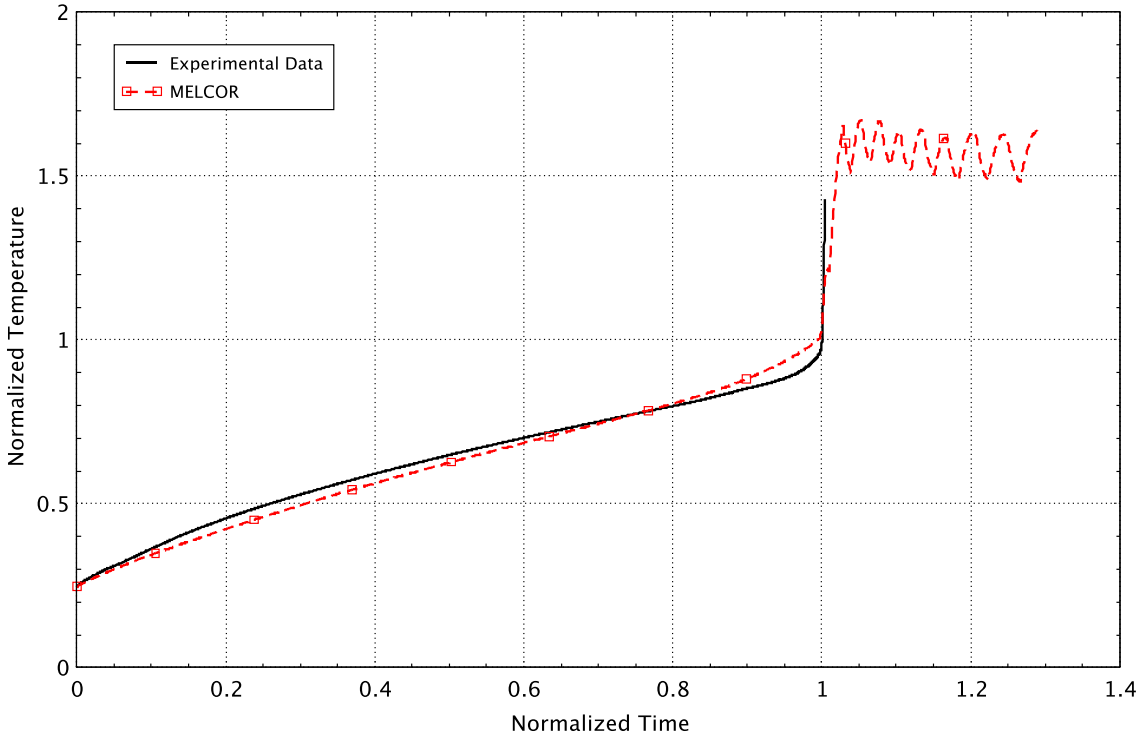

Figure 5. Peak cladding temperature versus time for the Phase 1 ignition test using cell 2

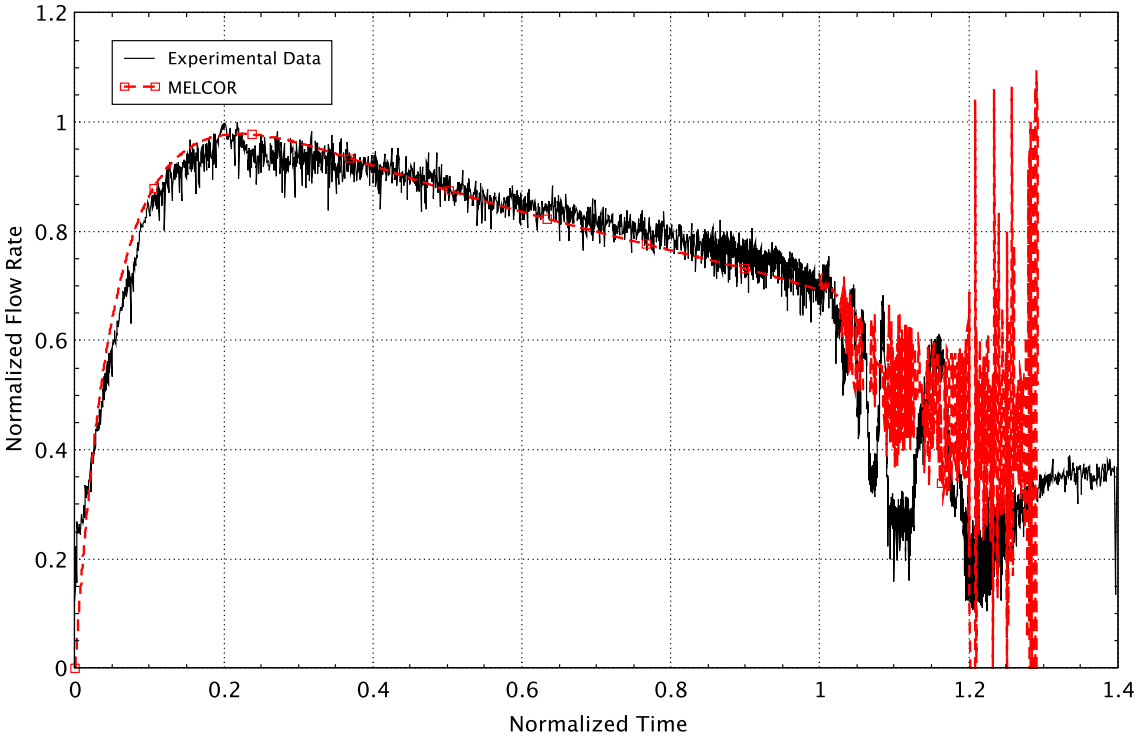

Figure 6. Volumetric flow rate versus time for the Phase 1 ignition test using cell 2

4.2 Phase 2 results and analysis

The Phase 2 experiments presented a more challenging modeling scenario than Phase 1. As the central assembly heats up to ignition, the heat flux to the surrounding unheated assemblies results in a large temperature gradient across the peripheral assemblies. Figure 7 shows temperature contours across the assemblies at a fixed elevation and for different times during the ignition test. Figure 8 shows the experimental data temperature as a function of distance from the centerline shortly before ignition at an elevation near the middle of the assembly. As seen in this figure, the temperature profile in the center heated assembly is relatively flat, while there is a large gradient in the peripheral assemblies. This large temperature gradient is particularly significant given that oxidation is highly temperature dependent and the oxidation reaction generates heat that then contributes further to the burn.

When using MELCOR to simulate the Phase 2 experiments, a single core ring (with single representative temperature) may be acceptable in the center assembly (as it was for the Phase 1 analysis). However, researchers found that a single core ring for the fuel rods in the unheated assembly was insufficient in capturing the large temperature gradients observed in the experiment. If MELCOR were modeling the assembly with a single ring for the unheated peripheral region, the average cell temperature would be used in calculating the oxidation rate. This would significantly underestimate the oxidation that occurs in the unheated assembly and would, therefore, also underestimate the associated heat generation. This can be overcome by using several core rings in the unheated peripheral region; however, when scaling up to a full spent fuel pool, this would result in a very large model that is difficult to manage.

Consequently, researchers modified the MELCOR code to allow improved temperature refinement within a single radial ring by providing a means for the user to specify multiple fuel rod types within that ring. As modified, the user can now specify up to five fuel rod types in each radial ring. For example, in the peripheral region, a single fuel rod type can be used to represent just the row of rods closest to the rack that divides the center assembly from the peripheral assemblies. Additional rod types can be defined with coarser nodalization for rods as they move closer to the outer rack. The input for these new fuel rod types includes new inputs to specify mass fractions for each fuel type, mass fractions for each control rod type, and view factors between fuel rods. In the current analysis, the view factors, which are based on the geometry of the problem, were computed with a CFD pre-processor. Figure 9 shows one way the fuel rods can be divided when using a detailed 9-ring model. In the MELCOR 2-ring multiple rod model of the Phase 2 experiments, this same division was used where rods 1-4 are in core radial ring 1 and rods 5-9 are in core radial ring 2. Note that all four unheated peripheral assemblies are lumped together with no distinction possible, for example, between the north and south assemblies. All results presented below use the MELCOR 2-ring model with multiple rods/core ring.

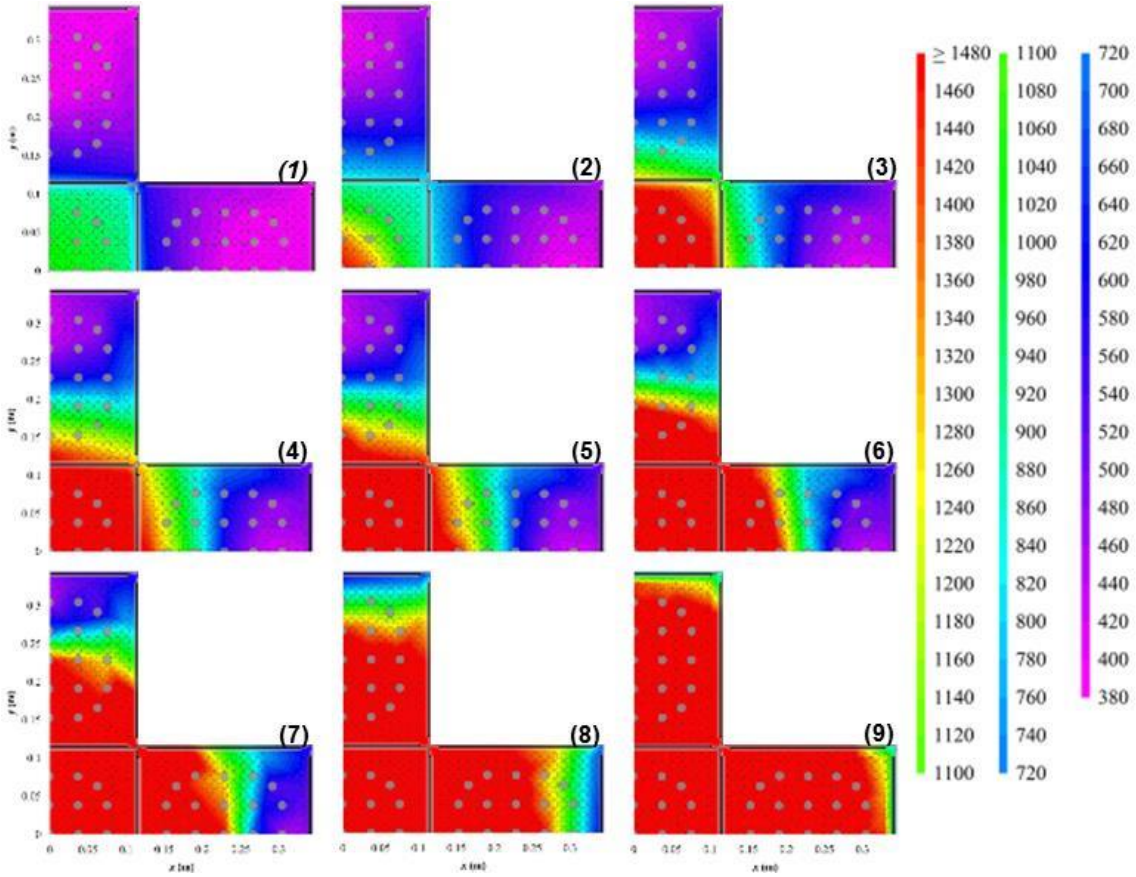

Figure 7. Temperature contours throughout the assemblies at different times during the Phase 2 ignition test

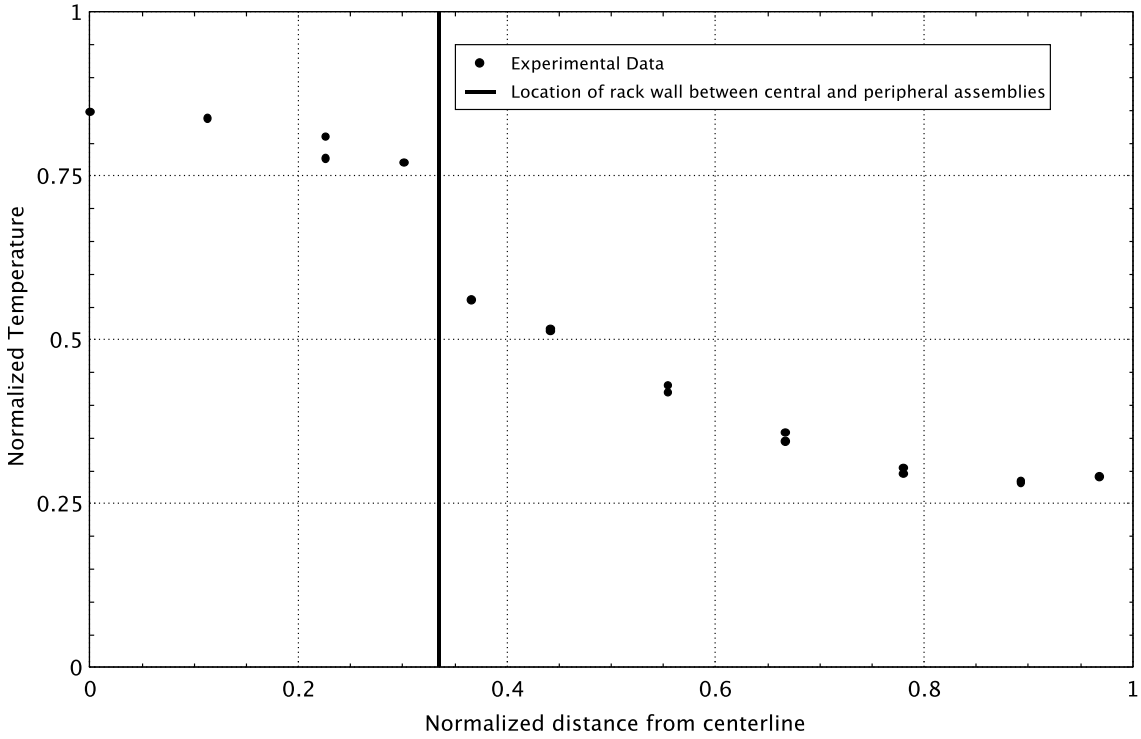

Figure 8. Radial temperature profile for the Phase 2 ignition test

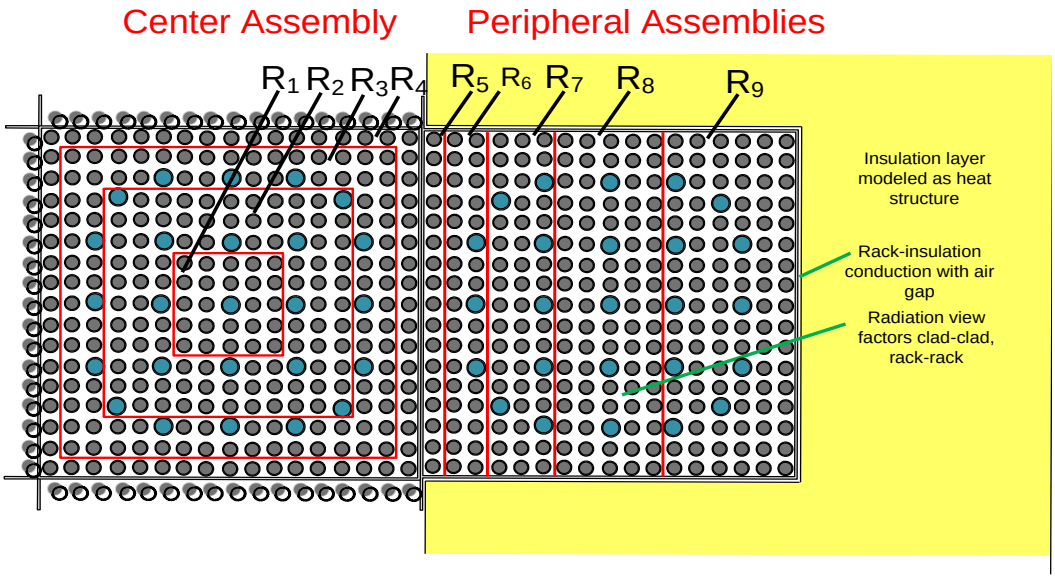

Figure 9. Fuel rod nodalization in the Phase 2 MELCOR model

Researchers successfully conducted nine Phase 2 pre-ignition tests, and they compared the MELCOR results to the experimental data. Similar to the Phase 1 pre-ignition tests, these experiments were run for a fixed time, or until the maximum temperature exceeded a certain threshold. Figure 10 shows temperatures in both the center and peripheral assemblies at an elevation approximately three-fourths the height of the assemblies. Note that the figure below

shows data for the experiments that ran to the set time and does not show the higher power cases that were terminated early because of high temperature. As seen in this figure, MELCOR shows good agreement for the maximum temperature in the center assembly, but it tends to over predict the average temperature. In the peripheral region, MELCOR tends to over predict the maximum temperature and is in good agreement with the average temperature.

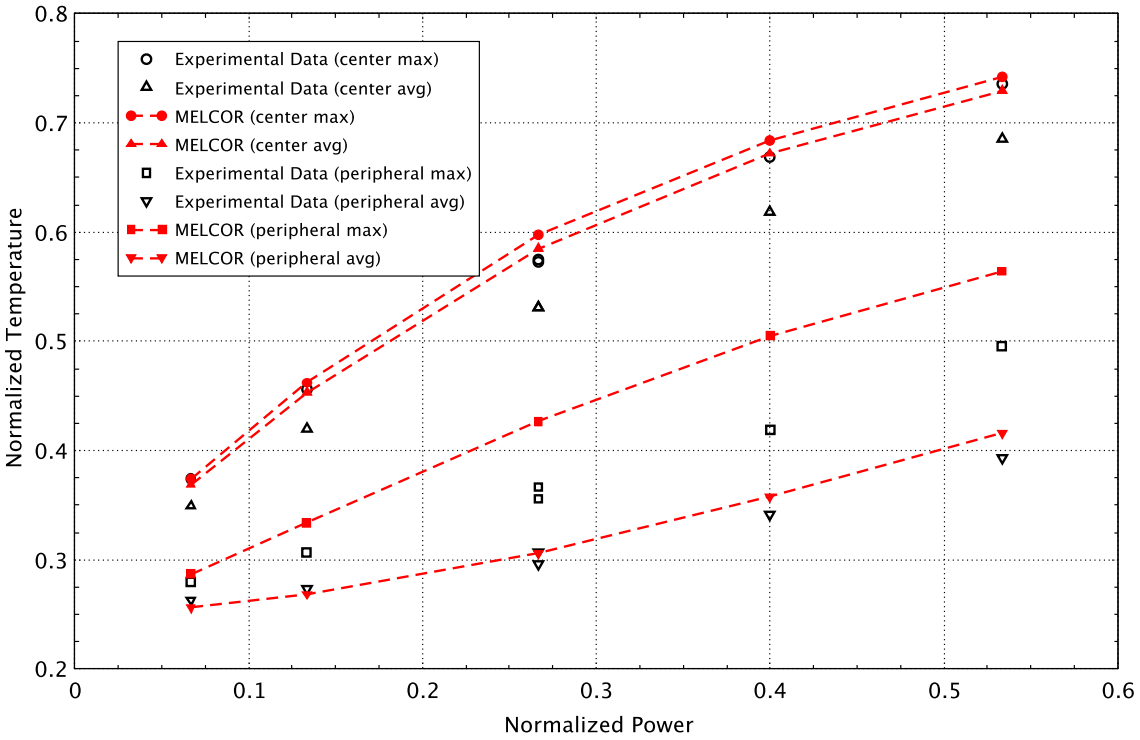

Figure 10. Temperature versus power for the Phase 2 pre-ignition tests

The Phase 2 experiment was successfully concluded with the ignition of the test assembly on June 6, 2012. Researchers surrounded the center assembly on four sides by unpowered, peripheral assemblies. Ignition of the Zircaloy within the center assembly was first observed at an axial level approximately three-fourths the height of the assembly. The burn front briefly propagated both upward and downward from this level but failed to reach the uppermost portion of the center assembly before becoming oxygen-starved. The ignition front primarily swept down the assembly toward the source of oxygen at the assembly inlet.

The first ballooning event in the pressurized, peripheral assemblies occurred shortly after ignition at a normalized time of 1.06, where the first occurrence of ignition in the center assembly occurs at a normalized time of 1.0. The Zircaloy fire first propagated into the peripheral assemblies at a normalized time of 1.12 at an elevation slightly below that of the center assembly. The ignition had progressed across the entire cross section of all of the peripheral assemblies at a normalized time of 1.4. Researchers' examination of the results revealed some degree of asymmetry in the propagation into the peripheral assemblies. As an example, the east assembly reached ignition approximately 0.04 normalized time units after the north assembly. This asymmetry is not ascribed to the ballooning events in the pressurized assemblies but is rather most likely caused by the limitations of construction and the chaotic nature of the Zircaloy fire. The ignition progressed to the bottom of the center assembly around

a normalized time of 2. All five fuel assemblies were completely consumed as a result of the Zircaloy cladding fire.

All of the pressurized fuel elements in the two pressurized, peripheral fuel bundles ballooned as a result of exposure to temperatures experienced during the ignition test. The ballooning events in the two assemblies occurred at approximately the same time at a given location, regardless of the initial pressure. Ballooning did not likely occur at a single axial level rather than over a range of elevations based on PCT data at the time each rod ballooned. The thermal-hydraulic behavior of assemblies with ballooned rods did not appear to be discernible from the unpressurized assemblies. Examination of the debris indicates that samples show a spectrum of ballooning events ranging from extreme tears in the cladding to localized gashes. All the samples show the additional effects of slumping, oxidation, and spallation.

Researchers used a residual gas mass spectrometer to monitor the concentrations of the gas constituents exiting the center assembly. The gas constituents monitored were nitrogen, oxygen, argon, water, carbon dioxide, and helium. Since argon and helium are inert noble gases and do not react with zirconium, the concentration of these gases relative to the reactive gas species provides a measure of the removal and release of the reactive gases. The analysis shows two distinct stages of oxidation over the course of the test. The primary oxidation stage was very energetic and continued until a normalized time of 1.7. During this stage, all the oxygen entering the assembly was consumed by oxidation of zirconium, and a substantial portion of the nitrogen was consumed by production of the nitride from much (if not most) of the remaining unoxidized zirconium. In a second oxidation stage, all of the oxygen entering the assembly was consumed by the oxidation of zirconium nitride, as indicated by the release of nitrogen gas. The additional release of energy from the wholesale production of zirconium nitride, coupled with the significant reduction in convective energy removal during the primary oxidation stage, are important phenomena to consider when assessing the propensity of an ignited assembly to propagate ignition to adjacent assemblies.

Researchers used several MELCOR models in the analysis of the Phase 2 experiments. These included a 2-ring model, a 9-ring model, and a 2-ring model with multiple rods/radial core ring. Results from the 2-ring with multiple rods/ring will be discussed below. The MELCOR model for Phase 2 used the same axial nodalization as the Phase 1 model, and increased the number of core radial rings from one in Phase 1 to two in Phase 2, in which the additional ring models the four unheated peripheral assemblies. The fuel rods were grouped as shown in Figure 9.

The MELCOR analysis showed that the results are highly sensitive to both oxidation kinetics and the transition to breakaway. Predicted time of ignition can vary up to several hours based on the selection of individual models and selected modelling parameters. When using the default oxidation kinetics and default lifetime model, ignition times were delayed up to several hours. However, when using the lower uncertainty (based on the 95-percent confidence level, as determined by the prediction band on the oxidation kinetics curve fit) in the lifetime model, MELCOR ignition times occurred before that of the experiment. Researchers found that the default MELCOR oxidation kinetics model was under-predicting the pre-breakaway oxidation heat, leading to delays in ignition. They modified the pre-breakaway oxidation kinetics to transition from a low- to high-temperature rate correlation, similar to what was done in the previous BWR study (NUREG-CR/7143). An additional case was run with a different oxidation model. The PSI oxidation model (Jonathan Birchley and Leticia Fernandez-Moguel, “Simulation of air oxidation during a reactor accident sequence: Part 1—Phenomenology and model development,” Annals of Nuclear Energy 40 (February 2012), pp. 163–170) uses pre-breakaway parabolic kinetics similar to the default MELCOR model. It also includes the use of oxide

thickness, linear kinetics, accelerated linear kinetics, and a transition phase. MELCOR results for four cases are shown below, including: code defaults, lower uncertainty on lifetime model, modified pre-breakaway oxidation kinetics, and the PSI oxidation model.

Figures 11 and 12 show the peak cladding temperature for the Phase 2 experiments for the central and peripheral assemblies, respectively. Figures 13 and 14 show the burn propagation in the center and peripheral assemblies, respectively. As seen in these figures, MELCOR results compare very favorably to the experimental data when using the modified pre-breakaway oxidation kinetics.

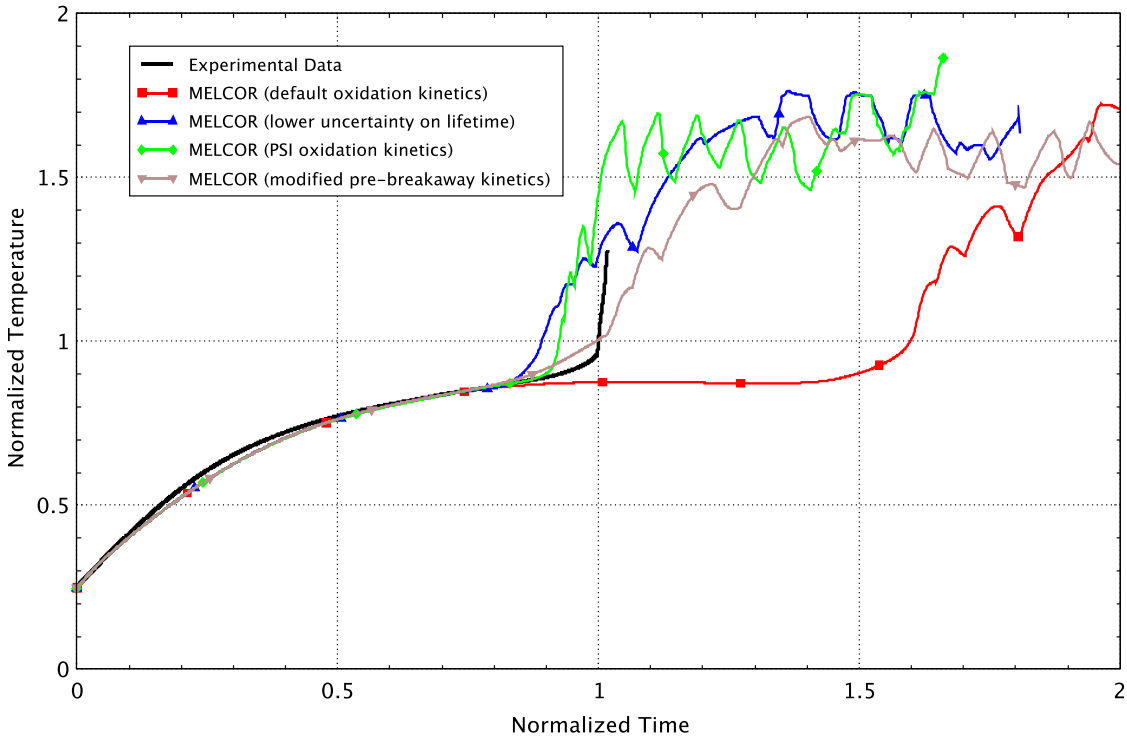

Figure 11. Peak cladding temperature in the center assembly for the Phase 2 ignition experiment

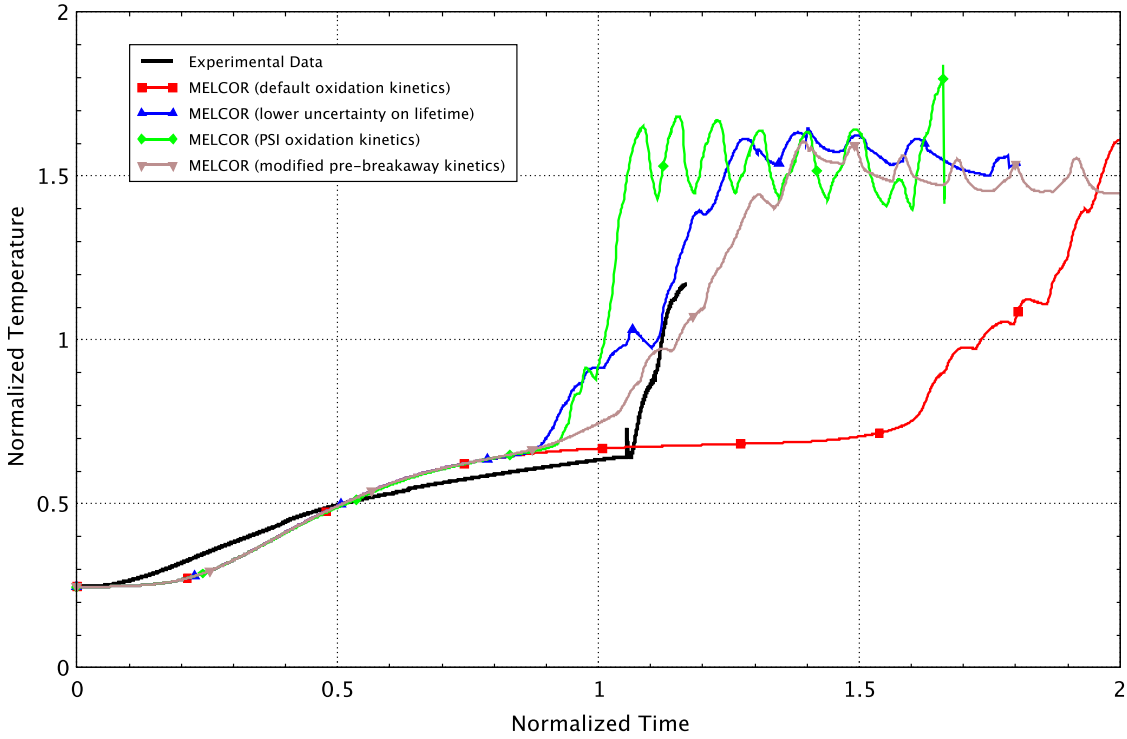

Figure 12. Peak cladding temperature in the peripheral assemblies for the Phase 2 ignition experiment

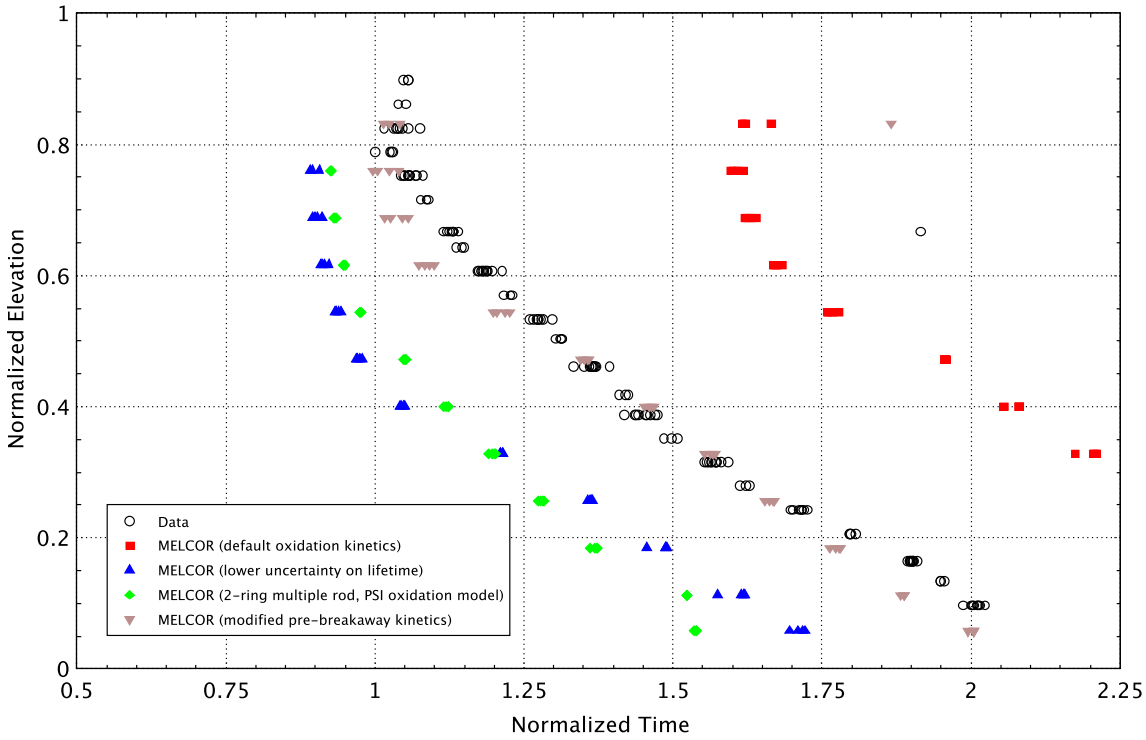

Figure 13. Central assembly ignition propagation for the Phase 2 ignition test

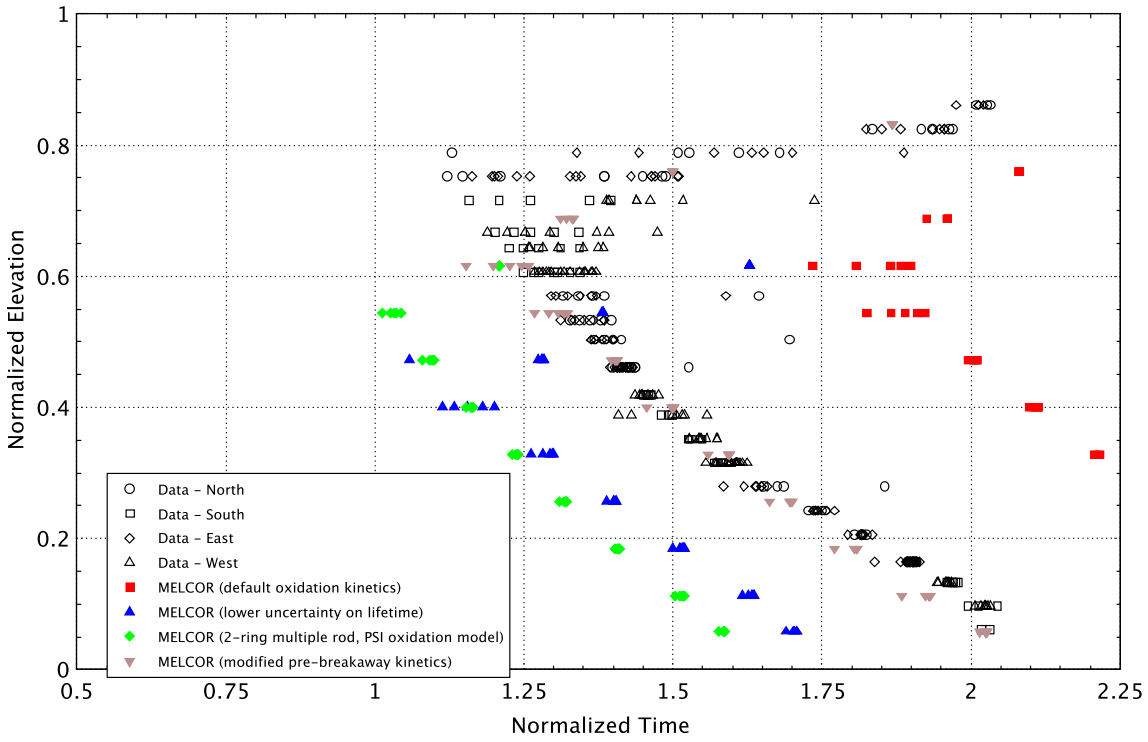

Figure 14. Peripheral assembly ignition propagation for the Phase 2 ignition test

5. Summary

Researchers successfully completed the OECD/NEA Spent Fuel Pool Project. They performed the project in two phases, with the objective to conduct a highly detailed thermal-hydraulic characterization of a full-length commercial fuel assembly mockup and provide data for the direct validation of severe accident computer codes (i.e., ATHLET-CD, ASTEC, DRACCAR, and MELCOR) during a PWR SFP under complete loss-of-coolant conditions. Phase 1 focused on axial heating and burn propagation, while Phase 2 addressed axial and radial heating and burn propagation, including effects of fuel rod ballooning. For each phase, testing included unheated flow tests, pre-ignition tests, and a final destructive ignition test.

Test assemblies representing full-length commercial 17x17 PWR fuel bundles were constructed using prototypic, commercial components with heater rods made from zirconium alloy tubing supplied by an industrial vendor. The test assemblies were fully instrumented, including hot wire anemometers (flow rate), oxygen sensors, mass spectrometer (argon and nitrogen gas quantification), quartz light pipes (visual observation of ignition), laser Doppler anemometer (velocity), pressure transducers, and thermocouples. In Phase 1, the test assembly was completely insulated to model boundary conditions, representing a “hot neighbor” loading pattern. In Phase 2, the center heated assembly was surrounded by four unheated peripheral assemblies representing “cold neighbor,” 1x4 loading pattern.

Researchers successfully completed all testing for both Phase 1 and Phase 2, and they generated valuable experimental data. The experimental data were then used to validate severe accident codes. MELCOR results showed excellent agreement to the test data for

Phase 1. For Phase 2, initial MELCOR results with a 2-ring model did not capture the large temperature gradient seen in the experiment. Code modifications were made to MELCOR, which increased the number of fuel rod components available in a single ring and allowed the user to simulate the test with much greater fidelity. The MELCOR analysis showed that the results are highly sensitive to oxidation kinetics and the transition from pre- to post-breakaway. Predicted time of ignition can vary up to several hours based on the selection of individual oxidation models and selected modelling parameters. Tests found that the default MELCOR oxidation kinetics model was under-predicting the pre-breakaway oxidation heat, leading to delays in ignition. Researchers modified the pre-breakaway oxidation kinetics to transition from a low- to high-temperature rate correlation, similar to what was done in the previous BWR study. Overall, results from the code validations demonstrate that MELCOR is capable of simulating PWR fuel with a complete loss of coolant.

Acknowledgment

The authors would like to acknowledge the following entities from 13 countries for their sponsorship and participation in the experimental program: the Nuclear Research Institut of the Czech Republic; the French Institut de Radioprotection et de Sûreté Nucléaire, Electricité de France; the Gesellschaft für Anlagen- und Reaktorsicherheit (GRS) mbH and Karlsruhe Institute of Technology, Germany; the AEKI Research Institute, NUBIKI Nuclear Safety Research Institute, jointly with the Paks Nuclear Power Plant, Hungary; the University of Pisa, Italy; the Japan Nuclear Energy Safety Organization; the Korea Atomic Energy Research Institute jointly with the Korea Institute for Nuclear Safety; the Institute for Energy Technology, Norway; the Consejo de Seguridad Nuclear and CIEMAT, Spain; the Swedish Radiation Safety Authority (SSM); the Paul Scherrer Institute, Switzerland; and the Health and Safety Executive, United Kingdom. Support from SNL Project Manager Ken B. Sorenson ensured the success of the experiments. Energy Research, Inc., developed the MELCOR model, and the required MELCOR code modifications and analysis would not have been possible without the support of Larry Humphries of SNL.